Turbulent dynamics inside the cavity of hot flow anomaly

P. Kovács[a,*], G. Facskó[b,c], I. Dandouras[d]

[a] *Geological and Geophysical Institute of Hungary, Budapest, Hungary*
[b] *Finnish Meteorological Institute, Helsinki, Finland*
[c] *Geodetic and Geophysical Institute, RCAES, HAS, Sopron, Hungary*
[d] *University of Toulouse, UPS-OMP, UMR5277, IRAP (Institut de Recherche en Astrophysique et Planétologie), Toulouse, France*

Abstract

In this paper the turbulent dynamics of a hot flow anomaly (HFA) event is investigated. The HFAs are transient plasma disturbances generated by the interaction of the bow shock (BS) and a tangential discontinuity (TD) embedded in the solar wind. The typical changes of the plasma parameters inside HFAs (increased plasma temperature, low bulk velocity, increased magnetic fluctuations, etc.) have been thoroughly interpreted by the records of space missions (e.g. Cluster). It is shown that the level of the turbulent intermittency inside the HFA cavity can be monitored in terms of space and time by the fourth statistical moment of the temporal differences of the time-series, i.e. by their flatness. With the multi-spacecraft observations the intermittency in the plasma fluctuations can be revealed not only in temporal but also in spatial scales. However, in the analysis, it must be taken into account that the dynamics of the foreshock region and the HFAs is governed not only by turbulent fluctuations but also by regular wave phenomena. In many cases the wave activities are more energetic than the turbulent processes, therefore the periodic signal components considerably modify the power-law behaviour of the turbulent spectra and determine the probability density functions and structure functions of the magnetic records exhibiting turbulent intermittency. On the other hand, while the wave phenomena are tight to certain time-scales, the turbulent character appears in a wide range of temporal scales. For this reason, it is argued that with the use of a dynamical high-pass filtering, the wave-like and turbulent-like components of the HFA magnetic signal can be discriminated. In our work the high-pass filtering is carried out with the use of continuous wavelet transformation. It is shown that the high-frequency components of HFA magnetic

*Corresponding author
Email addresses: kovacs.peter@mfgi.hu (P. Kovács), Gabor.Facsko@fmi.fi (G. Facskó), Iannis.Dandouras@cesr.fr (I. Dandouras)

fluctuations exhibit strong intermittency referring to turbulent dynamics. It is also suggested that in the low-frequency regime, the turbulent dynamics is hidden by the wave activities.

Keywords: hot flow anomaly, turbulence, probability density function, Cluster spacecraft, magnetic field

1. Introduction

In the middle of the 1980s anomalous hot plasma populations were discovered by the ISEE and AMPTE mission in the solar wind upstream of the terrestrial bow shock (Schwartz et al., 1985; Thomsen et al., 1986). The observed transient plasma phenomena were characterized by decreased particle density, increased temperature, slow down and deflection of the bulk velocity, depression and enhanced fluctuation of the magnetic field as compared to the ambient solar wind parameters. Because of its hot nature and anomalous solar wind velocity flow direction the phenomenon was termed hot flow anomaly (HFA). It was shown that HFAs were always associated with tangential discontinuity embedded in the solar wind and occurred along the interaction line of the discontinuity and the bow shock (BS) (Thomas et al., 1991). The anomalous plasma regime evolves due to the $E = -v \times B$ motional electric field that focuses the particles streaming upstream from the BS surface towards the discontinuity plane. The above physical mechanism has already been evidenced by hybrid plasma simulation (Thomsen et al., 1991; Lin, 1997; Lin, 2002). The cavity formed by the anomalous plasma is often bounded by sharp compressed edge regions corresponding to shocked plasma. The diameter of the cavity is highly variable but it is in the order of a few Earth radii (Lin 2002; Facskó et al., 2009, 2010; Zhang et al., 2010). The first observations and simulation results indicated that the quasi-parallel bow shock was the more favourable region for the generation of HFAs (Omidi and Sibeck, 2007; Facskó et al., 2009, 2010; Zhang et al., 2010), but recent studies evidenced the HFA occurrences upstream of quasi-perpendicular BS, as well (Wang et al., 2013 a,b).

On the basis of their typical properties, numerous HFA events have been identified and analysed on the records of AMPTE UKS, AMPTE IRM, ISEE 1 and 2, Interball (Schwartz et al., 1988, 2000), and Cluster spacecraft (Lucek at al., 2004; Kecskeméty et al., 2006; Facskó et al., 2009, 2010). Schwartz et al. (2000) have shown that the formation of HFA is most favoured if the motion of the underlying current sheet along the BS is slow, i.e. when the reflected ions have enough time to interact with the discontinuity plane. Moreover, they have also emphasized that the

electron and proton distribution inside the HFAs are nearly Maxwellian exhibiting strong contrast from that of the neighbouring plasma populations in the magnetosheath or the solar wind. In the analysis of different HFA events, Lucek et al. (2004) later confirmed that the distribution of particle population strongly depends on the time passed away from the beginning of the interaction between the TD and BS. In early stage of the HFA development two distinct ion populations are present corresponding to the incoming and reflected solar wind particles, whereas in the later phase the two populations develop to a single thermalized particle distribution through wave instabilities generating strong wave activities. The wave phenomena inside HFA cavities were investigated by Tjulin et al. (2008) using the k-filtering technique. They showed complex wave field in the young while uniform wave distribution in the more developed HFA events. With the statistical analysis of more than 120 HFA events recorded by the Cluster space mission Facskó et al. (2009) verified many of the theoretical predictions obtained from hybrid plasma simulation of Lin (2002). They confirmed e.g. the functional relations of the size of the HFA with the direction change of the magnetic field across the TD, or the angle between the TD normal and the Sun-Earth axis. Moreover, clear statistical evidences were found for the increasing probability of HFA occurrences with the increasing of the solar wind speed and Mach number.

Most of the papers related to HFA dynamics emphasized the strong and seemingly irregular fluctuation of the magnetic field in the core region of HFA cavity, that were attributed in many cases to turbulent activity. The turbulent character of the fluctuations appear in the intermittent bursts of the time-series (magnetic or velocity) of the anomalous processes. The intermittency can be quantitatively observed through the scale-dependent non-Gaussian statistics and long tails of the probability density functions (PDF) of incremental time-series of the turbulent signal over different scales. Since the turbulence is a multi-scale process, the non-Gaussian behaviour is obviously apparent in a wide range of temporal and spatial scales. In this paper, we argue however, that for the case of hot flow anomalies, certain time and spatial scales are dominated by wave activities (see papers of Tjulin et al. 2008, or Lucek et al., 2004) over the turbulent features. For this reason we were forced to limit the study of turbulent features to scales that are free from the wave phenomena.

2. Observation

In the present analysis we investigate the HFA event that was recorded by all of the Cluster spacecraft in 4th of January, 2007 between 05:07:00 and 05:10:00 UT. The event was selected from

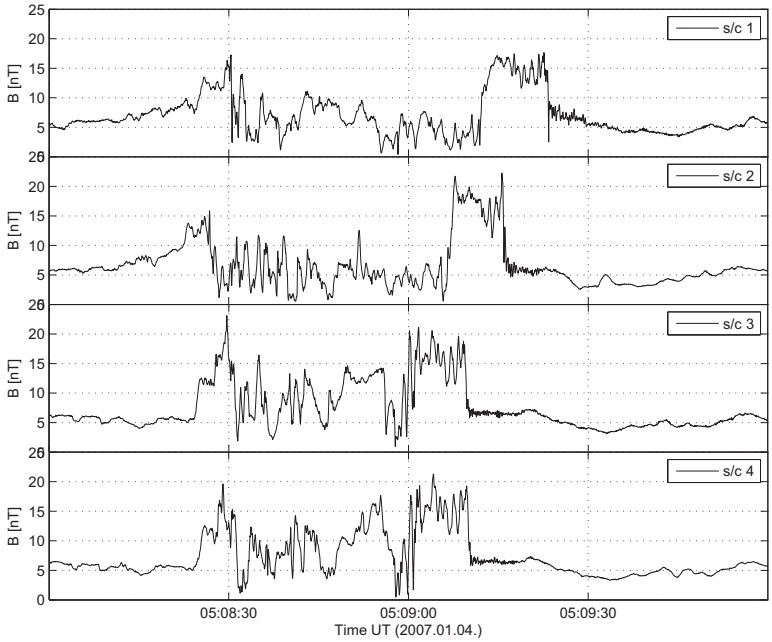

Figure 1: The total magnetic field variation during the investigated HFA event in the four spacecraft of the Cluster mission.

the list of HFA observations published by Facskó et al. (2009). In the time of the HFA record, the centre of the Cluster tetrahedron was in the (10.46, 11.44, -10.97) RE GSE position. The highest, lowest and mean separations between the spacecraft-pairs were 11220 km, 371 km, and 7105 km, respectively. The mission crossed the bow shock outbound before the anomaly and was moving toward the northern hemisphere in quasi-perpendicular solar wind environment when the HFA event was observed.

For the study, we used the 22,5 Hz frequency total field magnetic observations of the FGM instruments (Balogh et al., 1997) of the four s/c spacecraft (Fig. 1.). The records clearly show the period of the HFA event. The anomaly lasted between about 40-50 s on the four s/c records that corresponded to about 4-5 RE size considering the mean solar wind speed around the HFA of about ~640 km/s. In all records, the anomaly was bounded by compressional shock regions both of its leading and trailing edges, in between the magnetic field became very irregular and dropped to lower value comparing to the surrounding solar wind observations. For the case of the HFA crossing of the s/c3 spacecraft the variations of the magnetic components in the GSE and polar coordinate

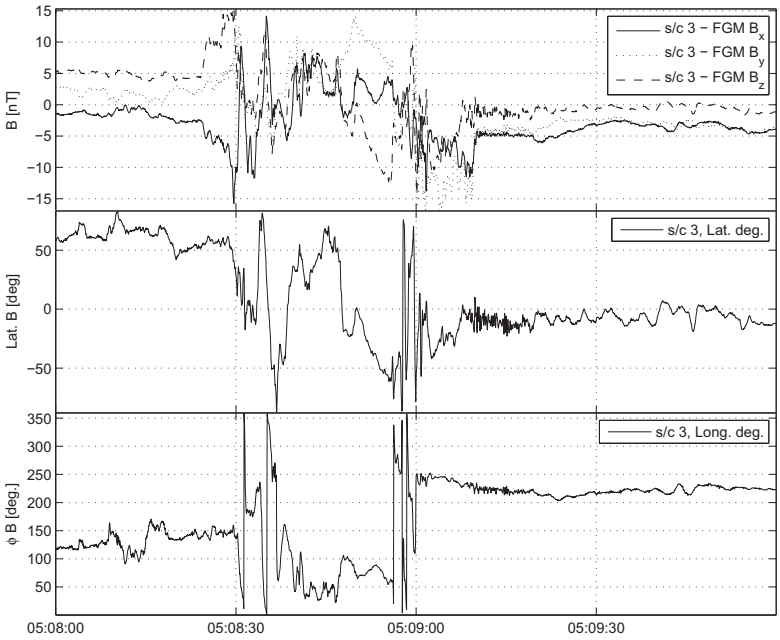

Figure 2: The magnetic variation during the investigated HFA event recorded by s/c 3 Cluster spacecraft in GSE x,y,z (upper panel) and polar (lower panels) coordinates.

systems are also presented (Fig. 2.). The polar representation evidenced that the magnetic field direction changed approximately 75° and 110° in latitude and longitude angle, respectively, in the core region of the anomaly. Supposing that the discontinuity was embedded in a plane, Facskó et al. (2009) have estimated n = [0.64, -0.64, 0.43] for its normal direction according to the cross product of the mean magnetic field recorded upstream and downstream of the HFA event. They have also estimated 113 degree overall rotation in the magnetic field direction between the upstream and downstream regions.

Lucek et al. (2004) suggested that according to the particle distributions inside the hot diamagnetic cavity early or developed stages of the anomaly evolution can be discriminated. The ion distributions of young HFAs exhibit clear separation between incident and reflected particles in the cavity. This state is, however, unstable and evolves to a homogeneous ion population, in association with significant wave activities. The more developed or mature HFAs, therefore, are characterized by single ion distribution. Zhang et al. (2010) investigated the variation of the electron spectrum in the centres of HFA cavities in terms of the anomaly evolution, and found that, unlike the spectra of young HFAs, there is a clear jump in the electron flux of the mature HFAs near 10 eV. Wang et al. (2013c) later confirmed this finding showing that the electron spectrum below and beyond the jump follows, respectively, Maxwellian and drift-κ distributions in the mature HFAs, while the young anomalies are represented by a single drift-κ distribution.

Zhang et al. (2010) also claimed that the strong compressional shock region at the cavity edges typically appear in the developed stage of the anomaly, i.e. in the cases of mature HFAs. Therefore, the clear enhancement of the magnetic field in the edge region of the studied HFA (Fig. 1.) might strongly indicate its mature character. On the other hand, according to the high- and low sensitivity CIS-HIA (Réme et al., 1997) record of the s/c 3 Cluster spacecraft we have also generated the $v_x - v_z$ velocity space distribution of the ion population inside the HFA cavity (Fig. 3.). In this plot the solar wind beam flowing in the negative X direction with velocity of approximately $-600km/s$ separates from the main ion population of the anomaly that is strongly scattered around the velocities of $v_x \approx 0km/s$ and $v_z \approx -1100km/s$. It implies the young nature of the anomaly. Finally, we have also checked the electron flux spectrum in the anomaly centre and compared it with that of observed before the HFA (Fig. 4.). The particle fluxes were measured by the PEACE instrument of the s/c2 Cluster spacecraft. The data recorded by the individual energy channels were normalized with the total flux observed in the whole energy range, both for

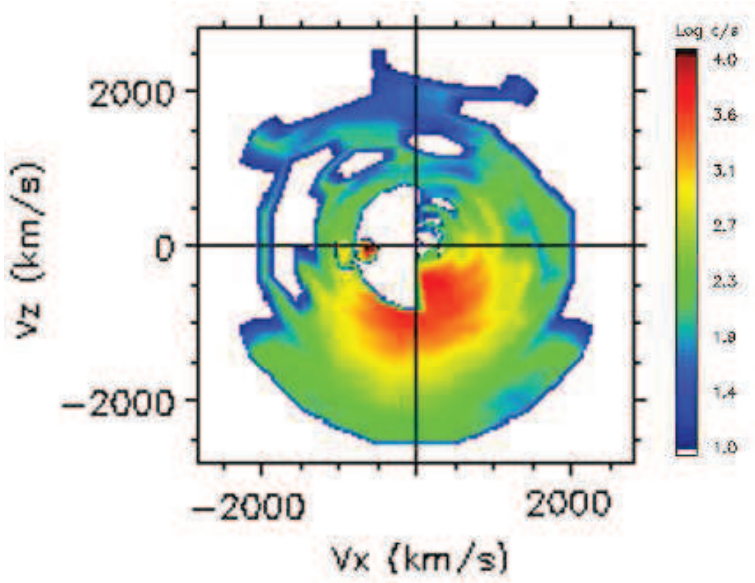

Figure 3: The high- and low-sensitivity $v_x - v_z$ velocity space distribution of the thermalized ion population observed by the CIS-HIA instrument of the s/c3 Cluster spacecraft in the centre of the studied HFA cavity (2007.01.04 05:08:40).

the cases of the HFA and the solar wind background. Clearly, the obtained HFA particle spectrum is similar in shape to that obtained by Wang et al. (2013c) for a young HFA (see Figure 7. of Wang et al. (2013c)); It does not exhibit sharp jump between the low and high energy parts, and in low energies ($< 25eV$) the flux rates are smaller, while in high energies are greater than that of measured in the background solar wind. In conclusion, the observed compressional shock at the cavity edges shown by the strong enhancement of the magnetic field and the obtained particle distributions provided ambiguous indications regarding to the age of the anomaly. Nevertheless, we conjecture that according to the ion and electron distributions it is more reliable to state that the studied event is still under development, in association with strong wave activities.

3. Methodology

Our investigations concern the analysis of intermittent turbulent properties of an HFA event. The study is based on the 22.5 Hz resolution magnetic observations of the Cluster space mission obtained inside and around the HFA cavity. Intermittency is related to the breakup of the statistical

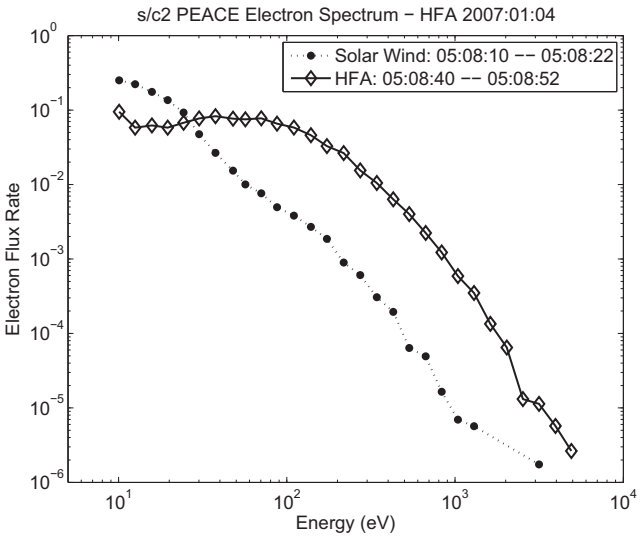

Figure 4: Electron spectrum measured by the PEACE instrument of the s/c2 Cluster spacecraft in the centre of the HFA cavity (diamonds) and in the neighbouring solar wind environment (dots) in 12 sec. temporal averages. The electron fluxes of the individual energy channels were normalized by the total flux measured in the whole energy band.

temporal and spatial self-similarity of the random turbulent velocity or magnetic field fluctuations. Self-similarity was suggested by Kolmogorov (1941) on the basis of dissipation-free, homogeneous energy-transfer along the inertial spatial and temporal scale range of the turbulent systems. In the case of real turbulent fluctuations intermittency manifests as randomly distributed, energetically powerful bursty events that can be observed in wide range of temporal scales. Although their occurrence may resemble to noisy pattern, the probability of bursts in the turbulent dynamics is much higher than it would be in the case of a Gaussian process. It means that the first and second order moments of turbulent time-series do not contain full statistical information on the underlying dynamics of intermittent turbulence, hence the higher order moments should be also investigated.

In this study our aim is to show that the magnetic pattern of hot flow anomaly events exhibits intermittency in certain time-scales, i.e. deviation from records of any Gaussian processes. For that, it is suggested that the $B_\tau(t) = B(t+\tau) - B(t)$ incremental time-series ($B(t)$ being the magnetic field time-series) represents the fluctuation pattern of the magnetic field across turbulent eddies of temporal scale τ. Intermittency can be evidenced by showing the scale-dependent deviation of the empirical probability density functions (PDF) of the incremental series from the Gaussian PDF

through the measurement of their kurtosis or flatness. The flatness, $F(\tau)$ is equivalent with the fourth statistical moment of the original incremental time-series:

$$F(\tau) = \frac{\langle B_\tau(t)^4 \rangle_t}{\langle B_\tau(t)^2 \rangle_t^2}, \quad (1)$$

The flatness of a Gaussian signal is 3. The rare but energetic intermittent events in the dynamical changes result in stretched PDFs associated with flatness higher than 3, while the lack of self-similarity in the intermittent dynamics involves their scale-dependency as well.

For the suitable investigation of the turbulent properties of the HFA dynamics it must be taken into account its (1) non-stationarity, (2) short duration and the (3) presence of considerable wave-activity. Obviously, the first two circumstances impede the study from statistical point of view by limiting the number of observations that relate to the investigated event. The problem can be partly overcome with sliding-window analysis in which moving overlapped sequences of the non-stationary signal are analysed separately and the obtained turbulent properties of each sequences are plotted in terms of time. This way, the trends in the variation of the turbulent behaviour over the investigated time-period can be demonstrated rather than exact results can be obtained regarding to the turbulent dynamics.

It is also obvious that the wave phenomena, if they exhibit bigger amplitude than the turbulent fluctuations, distort the statistical recognition of the turbulent properties through their strong effect on the elements of the incremental time-series in time-scales different from the wave periods. For this reason, in this study we applied a high-pass filtering to minimize the contribution of the wave components in the HFA magnetic signal. The filtering was carried out in the dynamical scale-time domain of the time-series generated by continuous wavelet transformation. For the transformation the Morlet mother wavelet had been used. Unlike the Fourier transformation, the wavelet decomposition allows one to investigate the coherent intermittent structures of turbulent dynamics (say, eddies) according to their position and size. Another favourable property of the wavelet transformation is that its resolution pattern fit to the cascade pattern of energy flow in turbulent dynamics (Farge et al., 1992), i.e. the coefficients of smaller scales are accompanied by better time resolution (i.e. localization) at the cost of looser frequency resolution and vice versa. The high-pass filtered time-series were obtained by the inverse wavelet transformation of only those wavelet coefficients that belonged to below a certain scale limit.

In order to check the reliability of the above technique in the analysis of non-stationary turbulent

signals superimposed with wave phenomena, we tested it in 10 minutes long synthetic time-series constituted of a Gaussian noise and two harmonic signals. The frequency-amplitude pairs of the harmonic components were $1/4$ Hz - 0.1 and $1/8$ Hz - 0.05 (arbitrary unit), while the added noise had maximum value of 0.1 (arbitrary unit). In the middle of the period (between 4-7 min.) an artificial intermittent turbulent signal was embedded that was constructed according to the multifractal P model introduced by Meneveau and Sreenivasan (1987). The model parameter was $P_1 = 0.75$. The signal was sampled by 22.5 sampling frequency. The wavelet filtering was carried out with cut-off period of 1 s, i.e. the harmonic components were totally filtered out. Fig.5 shows the original and filtered synthetic time-series, their wavelet scalograms and the results of their sliding-window probability density function analyses. The probability density functions and their flatness were computed for incremental time-series constructed with time scales of $\tau = 1, 5, 10s$, that intentionally differed from any of the periods of the harmonic components. The window width and its successive shift were $W = 30s$ and $S = 2s$, respectively. In the periods of 0-4 min and 7-10 min, i.e. when the intermittent turbulent fluctuations were still and already not present, the obtained flatness approached the value of 3 corresponding to the Gaussian noise, in the case of each temporal scale. It meant that the harmonic components did not influence the fourth statistical moments of the incremental time-series. Regarding to the intermittent part, the flatness curves of the original incremental signals exhibited a slight increase that corresponded to the strongest intermittency therefore lasted only for a short period. Intermittency was also evidenced by the increasing trend of the flatness towards the smaller scales, i.e. by the scale dependency of the PDFs. Considering the filtered signal, it turned out that the flatness curve exhibited an unambiguous increase during almost the whole period of the P model signal component, with a considerable peak around the strongest intermittency. It is noticed, however, that the decrease of the flatness with the lowering of the investigated scales was only apparent around the peak flatness values, and the neighbouring parts were characterized by ambiguous scale-dependency. Contrary to this finding, the obtained results affirm the conjectures that (1) the wave activity can drastically suppress the signatures of the background intermittent turbulence in the PDF analyses and that (2) the proposed high-pass filtering is suitable to enhance the effects of the intermittent processes in the analyses. It is argued that the efficiency of the technique lies in the multi-scale property of the turbulent dynamics whose fundamental signatures are apparent even in the high-frequency magnetic variations.

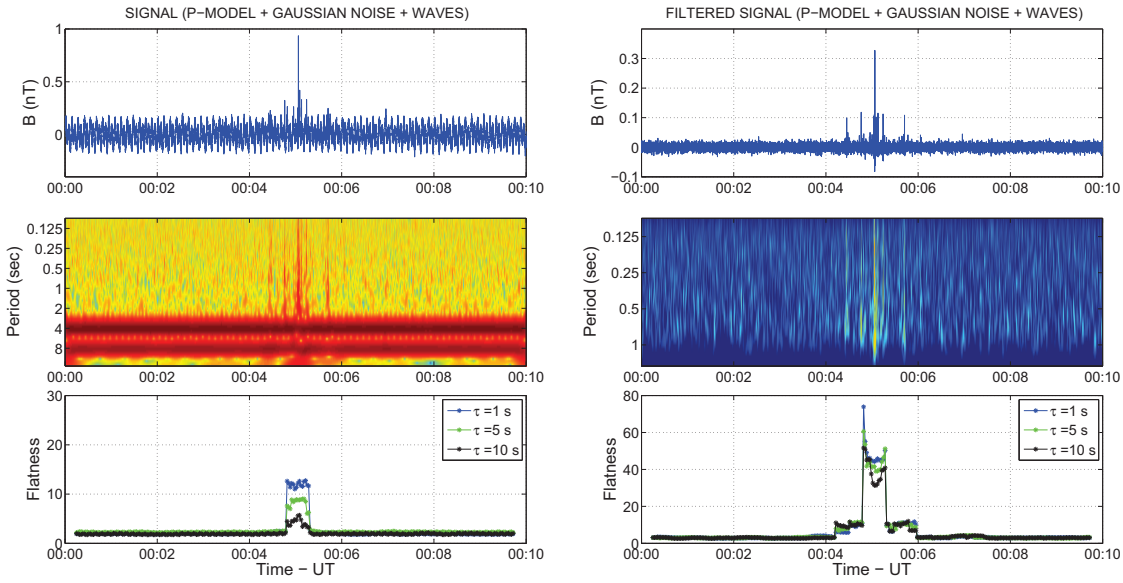

Figure 5: The synthetic intermittent time-series (see text) (top panels), their wavelet scalograms (middle panels), and the results of the sliding-window PDF analyses of the incremental signals, i.e. the variation of the flatness parameter in terms of time (bottom panels), for the time scales of $\tau = 1, 5, 10s$. The left and right panels refer to the original and high-pass filtered synthetic time-series, respectively.

4. Spectral analysis of the HFA magnetic record

In high Reynolds number flow systems the dissipation-free energy transfer among the inertial spatial scales prescribes the power-law behaviour of the velocity and magnetic field power spectral densities (PSD) with exponents of 5/3 (Kolmogorov, 1941) or 3/2 (Kraichnan, 1965) in HD or MHD turbulence, respectively. The solar wind is one of the classical examples for incompressible MHD environment where the above conjectures hold (e.g. Russel, 1972). Although, hot flow anomalies are located mostly in solar wind environment, ideal turbulent spectra for their variables cannot be expected, even in case of turbulent fluctuations in the cavities. Firstly, because the size of the HFA cavity is strongly limited in the direction perpendicular to the tangential discontinuity that prohibits the evolution of fully developed turbulence. Moreover, the presence and mixing of different plasma populations and also their interaction with the bow shock result in various instabilities and the appearance of wave phenomena that further distort the theoretical shape of the turbulent spectrum. Note, that these circumstances hold not only for the HFA dynamics but also for most of the plasma environment related to the planetary magnetosphere and their surroundings. It means that ideal turbulent spectra can be hardly experienced in the geospace environment.

Nevertheless, it is worth studying the spectral properties of the magnetic records of the HFAs, since they can show some essential hints regarding to the physical processes. The spectra of all of the Cluster records of the investigated HFA event exhibit similar features, therefore we present only the spectral result obtained from the observation of the s/c2 Cluster spacecraft. The power spectral densities (PSD) of the magnetic field were computed according to the Welch's (1967) method. In Fig. 6. we show the PSDs of 40 s long sequences of the time-series recorded between 05:08:30 - 05:09:10 and 05:07:00 - 05:07:40, i.e. before and inside the HFA cavity. The $PSD(f) \sim f^{-b}$ power-law character of the spectra is evident both in the anomaly and the solar wind. However, the HFA spectrum shows a spectral break at about the frequency of $f = 3\,Hz$. The exponents of the power-law spectra of the ambient solar wind and the HFA time-series in the low-frequency regime ($f < 3\,Hz$) are similar implying that the turbulent properties of the background fluctuations are modified dominantly in the high-frequency regime during the HFA period. It is emphasized that the common spectral exponent is close to that predicted by Kolmogorov (1941) for the spectra of neutral isotropic hydrodynamical turbulence.

Note, however, that the proton gyrofrequency inside the anomaly ($B \approx 5nT$) is about 0.08 Hz that means that almost the whole investigated frequency range can be classically attributed to the

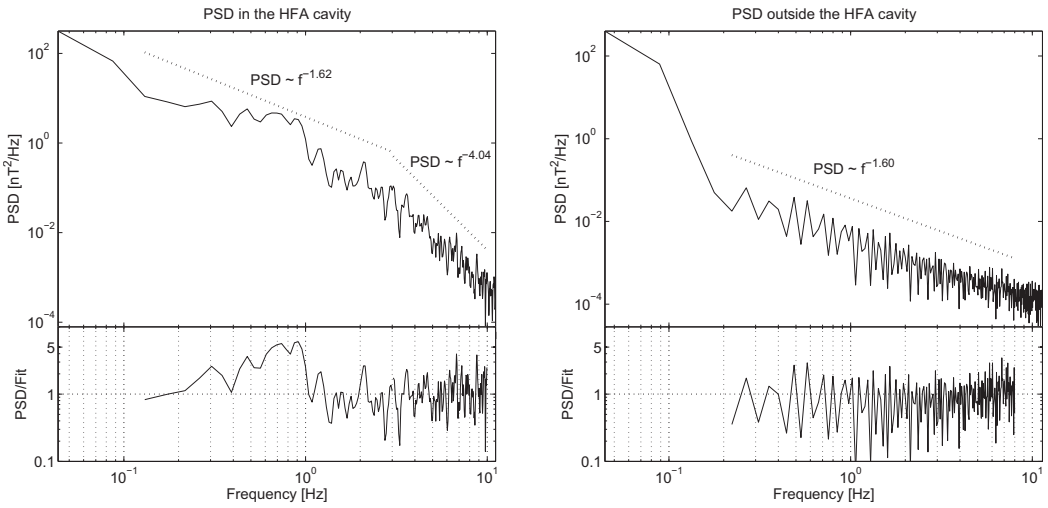

Figure 6: Power spectral density (PSD) of the magnetic field time-series recorded by the s/c2 spacecraft between 05:08:30 - 05:09:10 (left) and 05:07:00 - 05:07:40 (right), i.e. inside and before the HFA cavity. The bottom panels show the differences between the PSD and the fitted power-law curves.

dissipation range of turbulent dynamics. There is no clear observational evidence, however, that dissipative phenomena take place beyond the proton gyroscale (Alexandrova, 2008) in astrophysical plasmas. Instead, it is recently argued that the multi-scale turbulent processes can be interpreted in the frame of gyrokinetic description (Howes et al., 2008; Schekochihin et al., 2009), where the high-frequency fluctuations until the electron gyroscale are associated by a non-linear energy cascade governed by kinetic Alfvén waves (Bale et al., 2005), rather than by dissipative processes. An alternative explanation for the power-law spectrum beyond the proton gyroscale concerns with the fluid description of the turbulent phenomena and with the inclusion of the Hall term in the MHD equations (see Galtier and Buchlin, 2007 and references therein). In this case, the high-frequency electromagnetic fluctuations can be associated with nonlinear dispersive wave processes in which the whistler waves take the leading role. Note that according to the PEACE measurements of s/c2 spacecraft the mean ratio between parallel and perpendicular electron temperature in the investigated HFA centre was close to unity, therefore the driving of whistler waves was unrealistic.

In the low-frequency range of the HFA spectrum, the power-law approach fails to accurately fit the spectrum between about 0.4 and 1 Hz (see the bottom panel of Fig. 6.). The misfit is likely to

be caused by considerable wave activities associated with the HFA evolution (see Tjulin et al., 2008) and the heating of the plasma particles. Zhang et al. (2010) suggested that one of the possible candidates for electron heating in HFAs is the electrostatic lower-hybrid waves. Considering that the magnetic field amplitude in the investigated HFA is around 5 nT, the characteristic frequency of lower hybrid waves is about 3.2 Hz, that is near to the frequency of the spectral break. This finding would support the theory that beyond the spectral break a new cascade process emerges involving energy remnant after the considerable heating of plasma particles. The new cascade is characterized by a steep power-law spectrum exhibiting a scaling exponent of about -4.

From the comparison of the spectra of the solar wind and HFA time-series it is concluded that the basic spectral peculiarities of the HFA phenomenon are (1) the spectral break around the frequency of about $f = 3\,Hz$ and (2) the drastic steepening of the spectrum beyond the break. In order to check the robustness of these findings, the variations of the spectral exponents in the low ($f < 3\,Hz$) and high ($f > 3\,Hz$) frequency ranges were investigated in terms of time on the basis of a sliding window analysis. The s/c 2 time-series presented in Fig. 1. was divided into 30 seconds overlapping sequences for which the spectra and the fitted exponents in the two frequency bands were automatically computed and referred to the centre time of the sequences. The temporal variations of the exponents shown in Fig. 7. clearly evidence the change of the spectral property of the magnetic field in relation with the hot flow anomaly. It is also evidenced that while outside the anomaly the spectral slopes are similar in the two frequency bands, during the anomaly the power-law exponents, on the one hand, diverge from each other below and above $f \sim 3\,Hz$, on the other hand exhibit nearly constant values in the two ranges. The latter finding affirms the peculiar and stationary dynamics inside the anomaly.

5. Wavelet filtering and Sliding-window probability density function (SW-PDF) analysis of HFA time-series

Considering the average size of hot flow anomaly cavities of the order of some R_E (Earth radii) and the mean solar wind velocity of about 4-500 km/s, the expected duration of a HFA event in the spacecraft records is less than 1 minute. In the case of 22.5 Hz sampling frequency record it means about 1000 observations for any physical parameter, that is hardly enough for a careful statistical analysis focusing on rare intermittent events of turbulent dynamics. We therefore propose to carry out a sliding window (SW) turbulent analysis of the time-series that can track the change of the

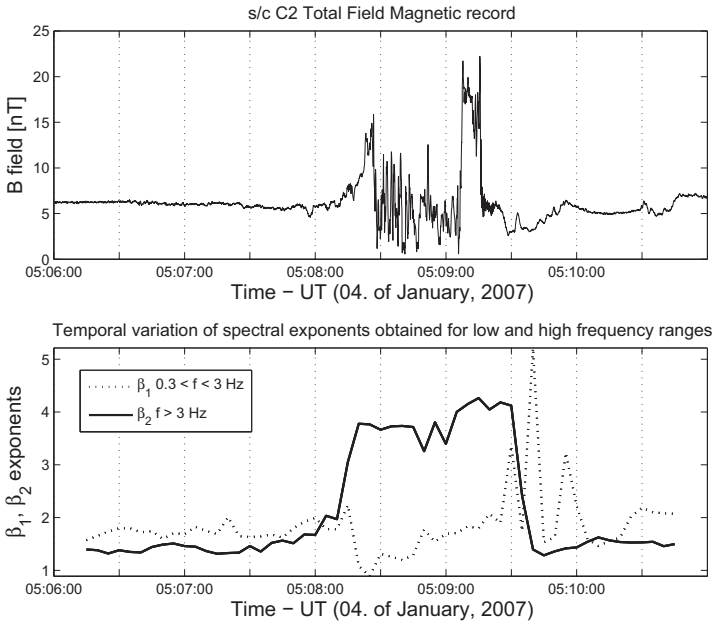

Figure 7: The magnetic field variation recorded by the s/c C2 Cluster spacecraft (top panel) and the temporal variation of the spectral exponents of the $PSD(f) \sim f^{-\beta}$ power-law fits obtained for the low ($f < 3\,Hz$, β_1) and high ($f > 3\,Hz$, β_2) frequency ranges of the spectra of 30 s overlapping sequences of the time-series (bottom panel).

turbulent parameters (e.g. flatness) from the downstream until the upstream part of the investigated HFA events. Note that this analysis is suitable for monitoring the variation of turbulent properties along a time-series, but not applicable for quantitatively characterizing the turbulent dynamics.

The turbulent flow is a spatio-temporal dynamical process in which numerous spatial structures (eddies) appear with different spatial extent. With single-spacecraft records, however, turbulence can be studied only in temporal scale, and for the spatial extensions of the results the Taylor hypothesis has to be invoked (Horbury, 2000). The multi-spacecraft missions, like Cluster, on the other hand provide unique opportunity for monitoring the simultaneous spatial fluctuation of the plasma properties among the spacecraft, as well. In this case the spatial scales and directions that can be studied are determined by the relative positions of the spacecraft participating in the mission.

In the following sections, we show the results of sliding-window probability density function analyses carried out with the use of temporal increments of single-spacecraft and spatial differences of simultaneous multi-spacecraft magnetic field records of the investigated HFA event.

5.1. Investigating the temporal field increments

The $B_\tau(t) = B(t+\tau) - B(t)$ temporal increment series of the magnetic records were computed with time scale of $\tau = 1, 5, 10s$. The window width and the time shift parameters of the sliding window analysis were $W = 30\,s$ and $S = 2\,s$, respectively. The results are summarized in Fig. 8. For the case of the original time-series (left panels of Fig. 8.) the fourth moments of the windowed incremental time-series (flatness) exhibit nearly Gaussian values upstream and downstream of the HFA, in all investigated time scales. In the leading and trailing parts, however, the PDFs of the incremental time-series seem to be increasingly non-Gaussian towards the smaller scales that is a clear signature of intermittent fluctuations in the compressional edges. The sliding PDF analysis of the central part of the HFA, on the other hand, relies on stochastic fluctuations in the higher temporal scales ($\tau = 5, 10s$), while it exhibits a moderate deviation from the Gaussian variations at the smallest scale ($\tau = 1s$).

On the basis of the synthetic analysis it was conjectured that the seemingly Gaussian statistics of an incremental time-series does not necessarily mean the lack of intermittency, but it can also be resulted in by harmonic wave components embedded in turbulent background. Therefore the filtering of the dominant wave components of the HFA signals that were apparent in their spectra

was indispensable for the investigation of the background noisy (probably turbulent) fluctuations.

From the spectral results it was concluded that the wave activity inside the investigated HFA could dominate the dynamical properties in frequencies below 3 Hz. For this reason the cut-off frequency of the high-pass filter process was set to 3 Hz. The filtered signals were obtained by the inverse wavelet transformation of wavelet coefficients belonging to temporal scales higher than 0.3 s. Evidently, the filtering suppresses a considerable part of the turbulent dynamics without which the full quantitative characterization of any of the underlying physical processes is not feasible. On the other hand, it is also supposed that the filtered time signal, void of wave components, can keep relevant information to statistically represent the turbulent properties of the system in high-frequencies, at least in a qualitative way.

The filtered signal, its wavelet scalogram and the result of its SW-PDF analysis is shown in the right panels of Fig. 8. As for the case of the original signal, the temporal increments were $\tau = 1, 5, 10s$. It is clearly seen from the temporal variation of the flatness that in the period of the HFA the PDF-s deviate considerably from the Gaussian, while in the upstream and downstream parts of the anomalous region the fluctuations remain stochastic, in all investigated scales. On the other hand, the scale dependency of the flatness does not show a clear evidence for increasingly non-Gaussian statistics of the incremental series with smaller and smaller scales during the anomaly, especially in the central region and the trailing edge of the HFA cavity. This finding is analogous with that obtained for the test analysis carried out with the filtered synthetic signal containing intermittent component. Thus, it is argued that the ambiguous scaling dependence of the PDFs of the real filtered time-series does not mean inevitably the lack of intermittency, but it is probably resulted in by the filter process, that drastically influences the multi-scale behaviour of the analysed signals.

We conclude then, that the filtering considerably enhances the non-Gaussian character of the HFA magnetic time-series and confirms the prevailing nature of intermittent multi-scale processes in the cavity. The strongest intermittency appears in the edges of the anomaly characterized by compressional shock. The PDF analysis carried out with spatial field differences also affirm these findings (see below).

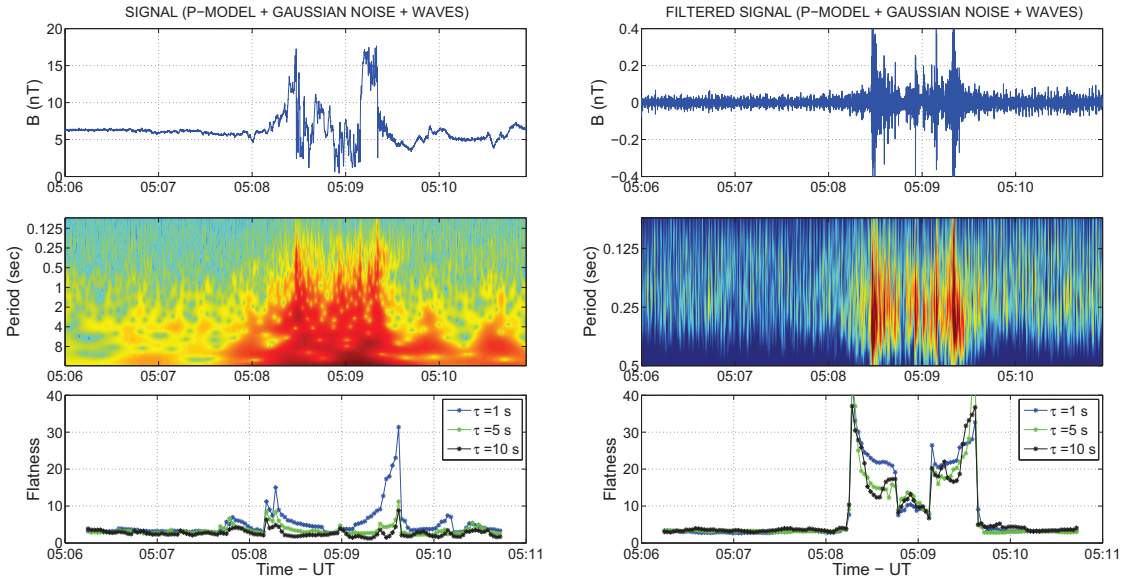

Figure 8: The analysed time-series (top panels), their wavelet scalograms (middle panels), and the results of the sliding-window PDF analyses of the records, i.e. the variation of the flatness parameter in terms of time (bottom panels), for the time scales of $\tau = 1, 5, 10s$. The left and right panels refer to the original and high-pass filtered HFA time-series recorded by the s/c1 Cluster spacecraft, respectively.

5.2. Sliding-window probability density function analysis of spatial field differences

The study of the turbulent fluctuations in spatial scales was carried out with time-series obtained by subtracting the simultaneously recorded magnetic field values of the six Cluster spacecraft-pairs. In order to avoid errors deriving from the different timings in the different spacecraft a three-samples moving average was applied on the new series. The six new signals represent spatial fluctuations in six scales and directions corresponding to the distances and directions among the spacecraft couples.

The time-series of spatial fluctuations were investigated by sliding-window probability density function analysis carried out with window with $W = 20\,s$ and time shift $S = 2\,s$. The temporal variation of the fourth moment (i.e. flatness) of the spatial fluctuation time-series were plotted by dotted curves on the graphs of Fig. 9 (each graphs correspond to one spacecraft couple). The spatial variations in the HFA cavity could depend on the spacecraft positions, inter-spacecraft distances and directions. The distances between spacecraft couples and their directions as compared to the normal of the tangential discontinuity related to the HFA (n = [0.64, -0.64, 0.43]) were indicated in the graphs. Unfortunately, the directional coverage of the spacecraft configuration was not uniform; it referred to 68-71° and 85° angles between the inter-spacecraft vectors and TD normal.

The black rectangles show the periods when both members of the analysed spacecraft couples were located between the compressional edges of the HFA, i.e. inside the diamagnetic cavity region. These periods are evidently shorter (between 30 and 40 s) than the HFA observation in one spacecraft, that demanded to set the window parameter of the SW analysis to 20 s instead of the previously applied 30 s. The flatness values in the common HFA periods are representative for the spatial field fluctuations in the anomaly. It is concluded that the dotted curves of these regions do not refer to any clear departure from the Gaussian statistics. The enhancement of the flatness around the cavity edges is the consequence of artificial singular values deriving from the subtraction of high and low magnetic values of the compressional and non-compressional regions.

Same analysis has been carried out with the high-pass filtered time-series that, contrary to the original series, suggests non-Gaussian spatial fluctuation in the HFA periods (continuous black curves). It means that beyond the frequency range of harmonic wave activities, i.e. in small temporal scales, the magnetic variations exhibit coherency among different spatial locations in the HFA cavity. The spacecraft configuration enables to investigate the field variation in spatial scales of about 300, 5000, 8000, 11000 km. The most straightforward enhancement of the non-Gaussian

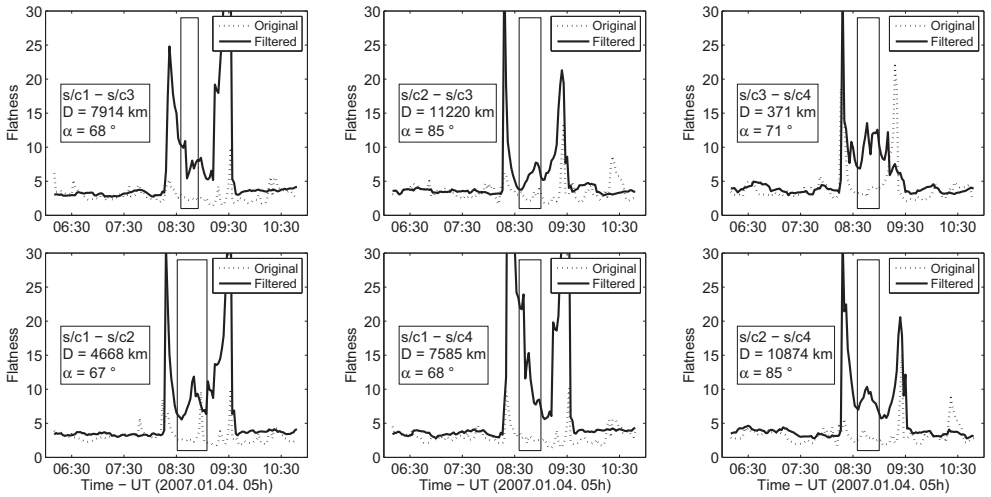

Figure 9: The variation of the flatness parameter in terms of time obtained from the PDF analysis of the spatial field differences of the six Cluster spacecraft couples. The black continuous and dotted curves indicate the flatness values obtained by the original and high-pass filtered time-series, respectively. The rectangles mean the periods when both members of the investigated spacecraft couples are in the HFA cavity region. The distances between the spacecraft couples and their orientations vs. the normal vector of the underlying tangential discontinuity are plotted in textboxes.

feature shows up in the case of the smallest scale, between spacecraft s/c3 and s/c4. On the other scales, the expected correlation between the flatness values and the spatial distances is not unambiguous. It is notable, however, that the fine structures of the flatness variations belonging to spacecraft-couples having similar distances and orientation (s/c1 or s/c2 vs. s/c3 and s/c4) are similar. The enhancement of the flatness values in the cavity edge regions is resulted in by the emergence of the sudden magnetic changes in the high-pass filter time-series. It is also noted that the orientations of the spacecraft-couples in terms of the TD normal do not exhibit any unambiguous relation to the non-Gaussian feature of the spatial field variation. It is emphasized however that the very narrow angle range of the orientations of spacecraft couples around the TD normal is not favourable for a thorough analysis of the anisotropic effects in the HFA cavity.

6. Summary and conclusion

In the paper, we have studied the turbulent properties of the magnetic fluctuations inside a hot flow anomaly observed by the Cluster mission. It was shown that the turbulent fluctuations of time-series (if exist) can remain hidden by wave activities appearing in the dynamical processes. For this reason, we proposed to carry out a high-pass filtering before the investigation of the turbulent behaviours of the time-series, e.g. by PDF analysis. The method was tested with synthetic time-series constituted of wave, noise and turbulent components. The spectrum of the studied HFA time-series exhibited power-law trend characterized by a spectral break and two distinct spectral slopes; about $\beta = -4$ at high ($f > 3\,Hz$) and about $\beta = -1.6$ at small ($f < 3\,Hz$) frequencies. The latter is close to the Kolmogorov spectral exponent of fully developed hydrodynamical turbulence. It was shown that in the low-frequency regime, the general power-law trend was strongly modified by wave activities, whose amplitudes were thought to be much higher than the average amplitude of the fluctuations generated by turbulent dynamics. On the other hand, in the high-frequency range of the magnetic variations, non-Gaussian temporal fluctuations could be evidenced by PDF analysis. Their intermittent nature was proven on the basis of the scaling dependence of the PDFs that was measured through the fourth moments of the incremental time-series, i.e. their flatness. Moreover, with the use of simultaneous spacecraft records inside the HFA cavity, the spatial coherency among the high-frequency plasma fluctuations obtained at the different spacecraft positions had also been verified. An important aspect is that for this finding the Taylor hypothesis predicting analogy between spatial and temporal physical variations in case of the study of high-velocity fluid stream had not to be invoked. We argue that the (1) well defined power law spectrum, (2) the deviation from the Gaussian statistics and its scale-dependence and (3) the spatial coherency of the high-frequency components of the HFA magnetic fluctuations referred to intermittent turbulent dynamical processes inside the HFA cavity.

It should however be emphasized that the observed turbulent properties had been identified for the frequency range that was beyond the f_{cp} proton gyrofrequency ($\sim 10^{-1}\,Hz$). In the classical approach of MHD turbulence the Alfvén type of fluctuations are suppressed by proton cyclotron damping at f_{cp}, thus the higher frequency processes are identified by dissipation phenomena. However, the dissipative dynamics is characterized by exponential fall-off of the PSD, in contrast to the observed power-law function of the HFA spectrum. Moreover, the non-Gaussian intermittent magnetic fluctuations existing even below the proton gyroscale also contradicts to the occurrence

of dissipative phenomena. As it was previously discussed, the "dissipation-scale" dynamics can be described in the frame of the gyrokinetic theory (Howes et al., 2008) or in association with the Hall MHD equations (Galtier and Buchlin, 2007). In both descriptions, the steepened power-law spectral regime beyond f_{cp} is resulted in by an energy cascade that is evolved from energies remnant after an inertial-range energy cascade governed by Alfvénic fluctuations. Thus, the observed cascade dynamics in the high-pass filtered magnetic fluctuations of the HFA indirectly implies the existence of turbulent cascading in smaller frequencies (higher scales), as well, where the wave activities upset the direct investigation of turbulence.

According to the ion velocity distribution and the electron spectrum it was claimed that the investigated anomaly event was young, though the clear compressional shock edges relied to its more developed stage. Since the different evolutionary phases of the HFAs are associated by different wave activities, it is suggested that the turbulent processes may also exhibit variation between the young and mature stages of the anomalies. The variation of turbulent properties in terms of the age of the HFAs will therefore need further studies.

Acknowledgements

The work was supported by the National Office for Research and Technology (Hungarian Space Office, grant number: URK09153), and by OTKA Grant (K 75640). The research leading to these results has also received funding from the European Community's Seventh Framework Programme ([FP7/2007-2013]) under grant agreement n° 313038/STORM. P. Kovács was supported by Bólyai Scholarship. G. Facskó was supported by ECLAT EU FP7 Project (Grant number 263325). Wavelet software was provided by C. Torrence and G. Compo, and is available at URL: http://paos.colorado.edu/research/wavelets/. Fig. 3 was created by the CL tool. We thank E. Penou at IRAP for software support. The authors acknowledge the use of the Cluster data to ESA Cluster Active Archive and the Cluster FGM (PI: E. Lucek), CIS (PI: I. Dandouras) and PEACE (PI: A. Fazakerley) instrument teams. We thank the reviewers for their suggestions and comments for improving the paper.

REFERENCES

[1] Alexandrova, O., Solar wind vs. magnetosheath turbulence and Alfvén vortices, Nonlin. Processes Geophys., 15, 95-108, 2008

[2] Bale, S.D., Kellogg, P.J., Mozer, F.S., Horbury, T.S., Reme, H., Measurement of the electric fluctuation spectrum of magnetohydrodynamic turbulence, Physical Review Letters, 94, 21, doi:10.1103/PhysRevLett.94.215002, 2005

[3] Balogh, A., Dunlop, M.W., Cowley, S.W. H., Southwood, D. J., Thomlinson, J. G., Glassmeier, K.-H., Musmann, G., Luhr, H., Buchert, S., Acuna, M., Fairfield, D. H., Slavin, J. A., Riedler, W., Schwingenschuh, K., and Kivelson, M. G., The Cluster magnetic field investigation, Space Sci. Rev., 79, 65-91, 1997.

[4] Biskamp, D.; *Nonlinear Magnetohydrodynamics*, Cambridge Univ. Press, Cambridge, 1993.

[5] Facskó, G., Z. Németh, G. Erdős, A. Kis, and I. Dandouras; A global study of hot flow anomalies using Cluster multi-spacecraft measurements, Annales Geophysicae, 27, 2057-2076, 2009.

[6] Facskó, G., J.G. Trotignon, I. Dandouras, E.A. Lucek, P.W. Daly; Study of hot flow anomalies using Cluster multi-spacecraft measurements, Advances in Space Research, 45, 4, pp. 541-552, 2010

[7] Farge, M., "Wavelet transforms and their applications to turbulence", Annu. Rev. Fluid Mech., 24, 395–457., 1992

[8] Galtier, S., É. Buchlin; Hall-MHD turbulence in the solar wind, Advances in Turbulence XI Springer Proceedings in Physics, 2007, Volume 117, 70-72, DOI: 10.1007/978-3-540-72604-3_20

[9] Horbury, T.S.; Cluster II analysis of turbulence using correlation functions. In: Harris, R.A. (ed.) Cluster-II Workshop Multiscale/Multipoint Plasma Measurements SP-449, ESA, Noordwijk, 89., 2000

[10] Howes, G.G., Cowley, S.C., Dorland, W, Hammett, G.W., Quataert, E., Schekochihin, A.A., A model of turbulence in magnetized plasmas: Implications for the dissipation range in the solar wind, Journal of Geophysical Research, 113, 1978-2012, doi:10.1029/2007JA012665, 2008.

[11] Kecskeméty, K., Erdős, G., Facskó, G., Tátrallyay, M., Dandouras, I., Daly, P., and Kudela, K.: Distributions of suprathermal ions near hot flow anomalies observed by RAPID aboard Cluster, Advances in Space Research, 38, 1587–1594, doi:10.1016/j.asr. 2005.09.027, 2006.

[12] Kolmogorov, A.N.; *Local structure of turbulence in an incompressible fluid at very large Reynolds numbers*, Dokl. Akad. Nauk SSSR **30**, 299-303, 1941.

[13] Kraichnan, R.H.; Inertial range spectrum in hydromagnetic turbulence, Phys. Fluids, **8**, 1385-1387, 1965.

[14] Lin, Y.; Generation of anomalous flows near the bow shock by its interaction with interplanetary discontinuities, J. Geophys. Res., 102, 24265-24281, 1997.

[15] Lin, Y.: Global hybrid simulation of hot flow anomalies near the bow shock and in the magnetosheath, Planetary and Space Sciences, 50, 577–591, 2002.

[16] Lucek, E.A., Horbury, T.S., Balogh, A., Dandouras, I., and Rème, H., Cluster observations of hot flow anomalies, Journal of Geophysical Research, 109, 6207, doi: 10.1029/2003JA010016, 2004.

[17] Meneveau, C., K.R. Sreenivasan; *Simple multifractal cascade model for fully developed turbulence*, Phys. Rev. Lett., **59**, 1424-1427, 1987a.

[18] Omidi, N., and D. G. Sibeck; Formation of hot flow anomalies and solitary shocks, J. Geophys. Res., 112, A01203, doi:10.1029/2006JA011663., 2007

[19] Réme, H. et al. The Cluster ion spectrometry (CIS) experiment. Space Sci. Rev. 79, 303, 1997.

[20] Russel, C.T., "Comments on the Measurements of Power Spectra of the Interplanetary Magnetic Field", in Solar Wind, (Eds.) Sonett, C.P., Coleman, P.J., Wilcox, J.M., Proceedings of a conference held March 21-26, 1971, at the Asilomar Conference Grounds, Pacific Grove, Calif., pp. 365-374, NASA, Washington, USA, 1972.

[21] Schekochihin, A.A., Cowley S.C., Dorland, W., Hammett, G.W., Howes, G.G., Quataert, E., Tatsuno, T., Astrophysical gyrokinetics: kinetic and fluid turbulent cascades in magnetized weakly collisional plasmas, The Astrophysical Journal Supplement Series, 182, doi:10.1088/0067-0049/182/1/310, 2009.

[22] Schwartz, S.J., C.P. Chaloner, P.J. Christiansen, A.J. Coates, D.S. Hall, A.D. Johnstone, M.P. Gough, A.J. Norris, R.P. Rijnbeek, D.J. Southwood, L.J.C. Woolliscroft; An active current sheet in the solar wind, Nature, 318, 269-271, 1985.

[23] Schwartz, S. J., R.L. Kessel, C.C. Brown, L.J.C. Woolliscroft, M.W. Dunlop, C.J. Farruggia, and D.S. Hall; Active current sheets near the Earth's bow shock, J. Geophys. Res., 93, 11295-11310, 1988.

[24] Schwartz, S. J., Paschmann, G., Sckopke, N., Bauer, T. M., Dunlop, M., Fazakerley, A. N., and Thomsen, M. F.: Conditions for the formation of hot flow anomalies at Earth's bow shock, Journal of Geophysical Research, 105, 12 639–12 650, doi:10.1029/ 1999JA000320, 2000.

[25] Thomas, V. A., D. Winske, M. F. Thomsen, and T. G. Onsager, Hybrid simulation of the formation of a hot flow anomaly, J. Geophys. Res., 96(A7), 11,625-11,632, doi:10.1029/91JA01092, 1991

[26] Thomsen, M.F., J.T. Gosling, S.A. Fuselier, S.J. Bame, and C .T Russell, Hot, diamagnetic cavities upstream from the Earth's bow shock, J. Geophys. Res., 91, 2961-29731, 1986

[27] Tjulin, A., E.A. Lucek, and I. Dandouras; Wave activity inside hot flow anomaly cavities, Journal of Geophysical Research, 113, A08113, doi: 10.1029/2008JA013333, 2008.

[28] Wang, S., Q. Zong, H. Zhang, Cluster observations of hot flow anomalies with large flow deflections: 1. Velocity deflections, Journal of Geophysical Research, 118, 732-743, doi:10.1002/jgra.50100, 2013a

[29] Wang, S., Q. Zong, H. Zhang, Cluster observations of hot flow anomalies with large flow deflections: 2. Bow shock geometry at HFA edges, Journal of Geophysical Research, 118, 418-433, doi:10.1029/2012JA018204, 2013b

[30] Wang, S., Q. Zong, H. Zhang, Hot flow anomaly formation and evolution: Cluster observations, Journal of Geophysical Research, 118, 4360-4280, doi:10.1002/jgra.50424, 2013c

[31] Welch, P.D, "The Use of Fast Fourier Transform for the Estimation of Power Spectra: A Method Based on Time Averaging Over Short, Modified Periodograms," IEEE Trans. Audio Electroacoustics, Vol. AU-15 (June 1967), pp.70-73., 1967.

[32] Zhang, H., D.G. Sibeck, Q.-G. Zong, S.P. Gary, J.P. McFadden, D. Larson, K.-H. Glassmeier, V. Angelopoulos, V.; Time History of Events and Macroscale Interactions during Substorms observations of a series of hot flow anomaly events, J. Geophys. Res., 115, A12235, doi:10.1029/2009JA015180, 2010

Figure1

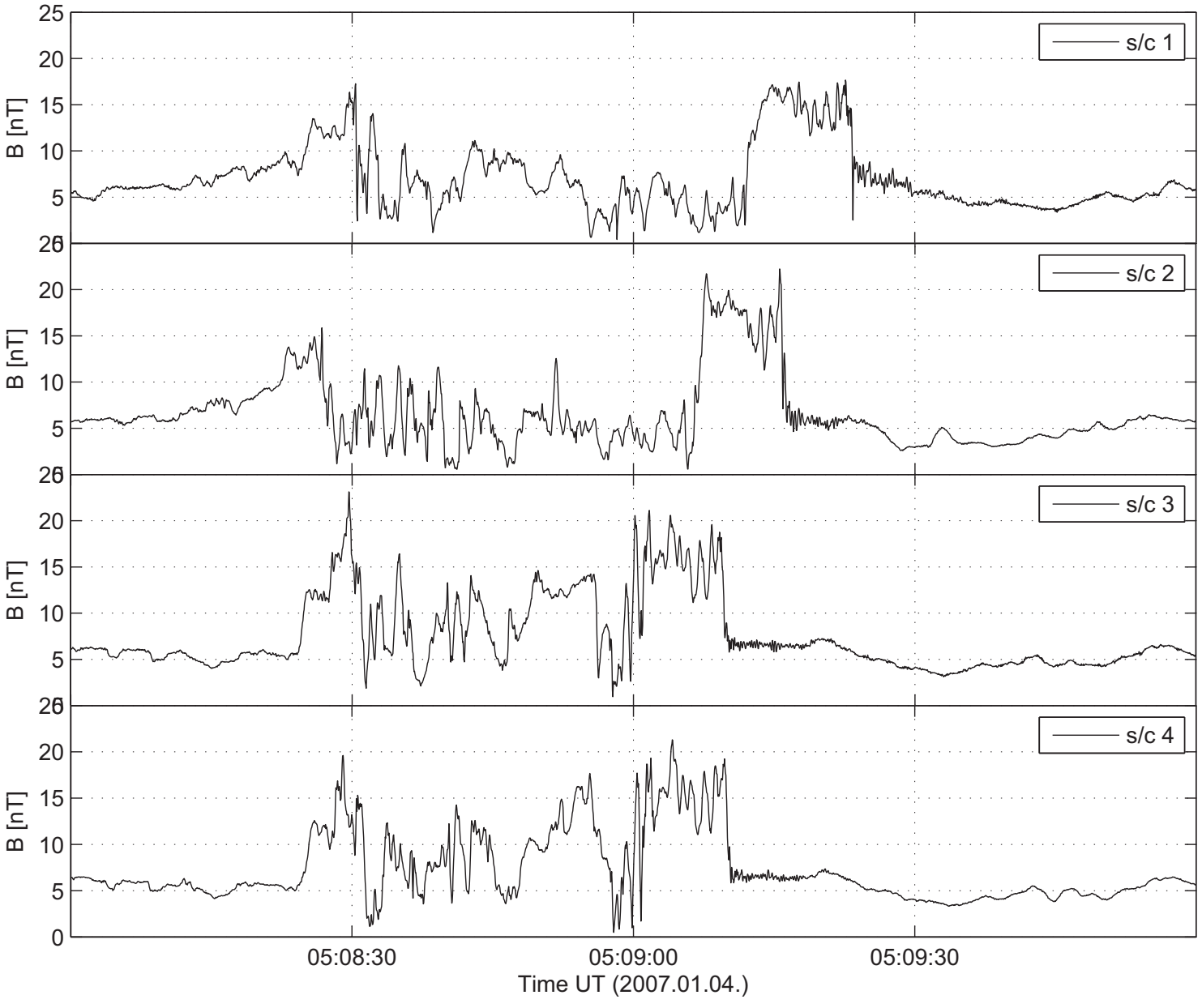
s/c 1
s/c 2
s/c 3
s/c 4
B [nT]
25
20
15
10
5
0
05:08:30
05:09:00
05:09:30
Time UT (2007.01.04.)

Figure2

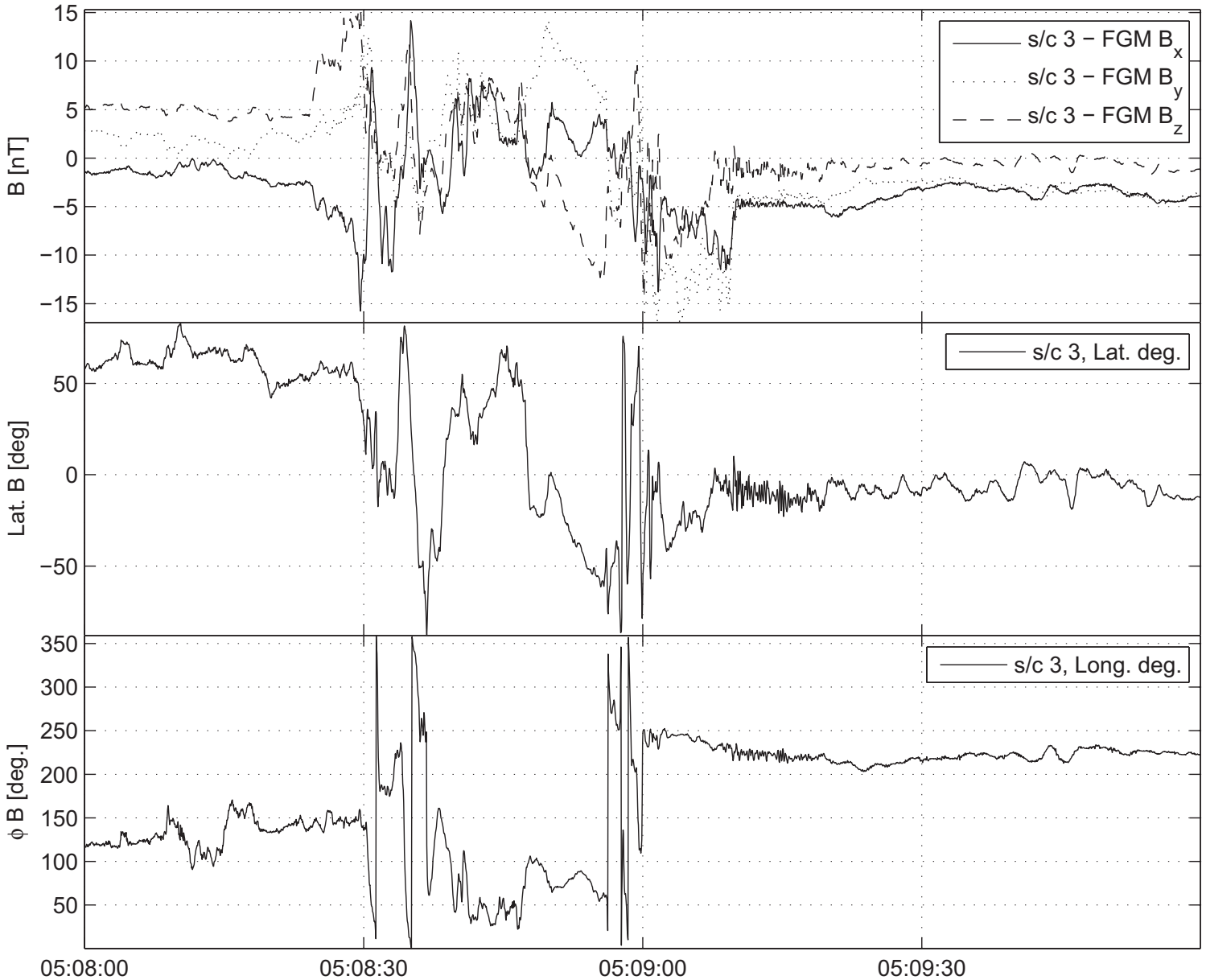
B [nT]
15
10
5
0
−5
−10
−15
s/c 3 − FGM B_x
s/c 3 − FGM B_y
s/c 3 − FGM B_z
Lat. B [deg]
50
0
−50
s/c 3, Lat. deg.
ϕ B [deg.]
350
300
250
200
150
100
50
s/c 3, Long. deg.
05:08:00
05:08:30
05:09:00
05:09:30

Figure3

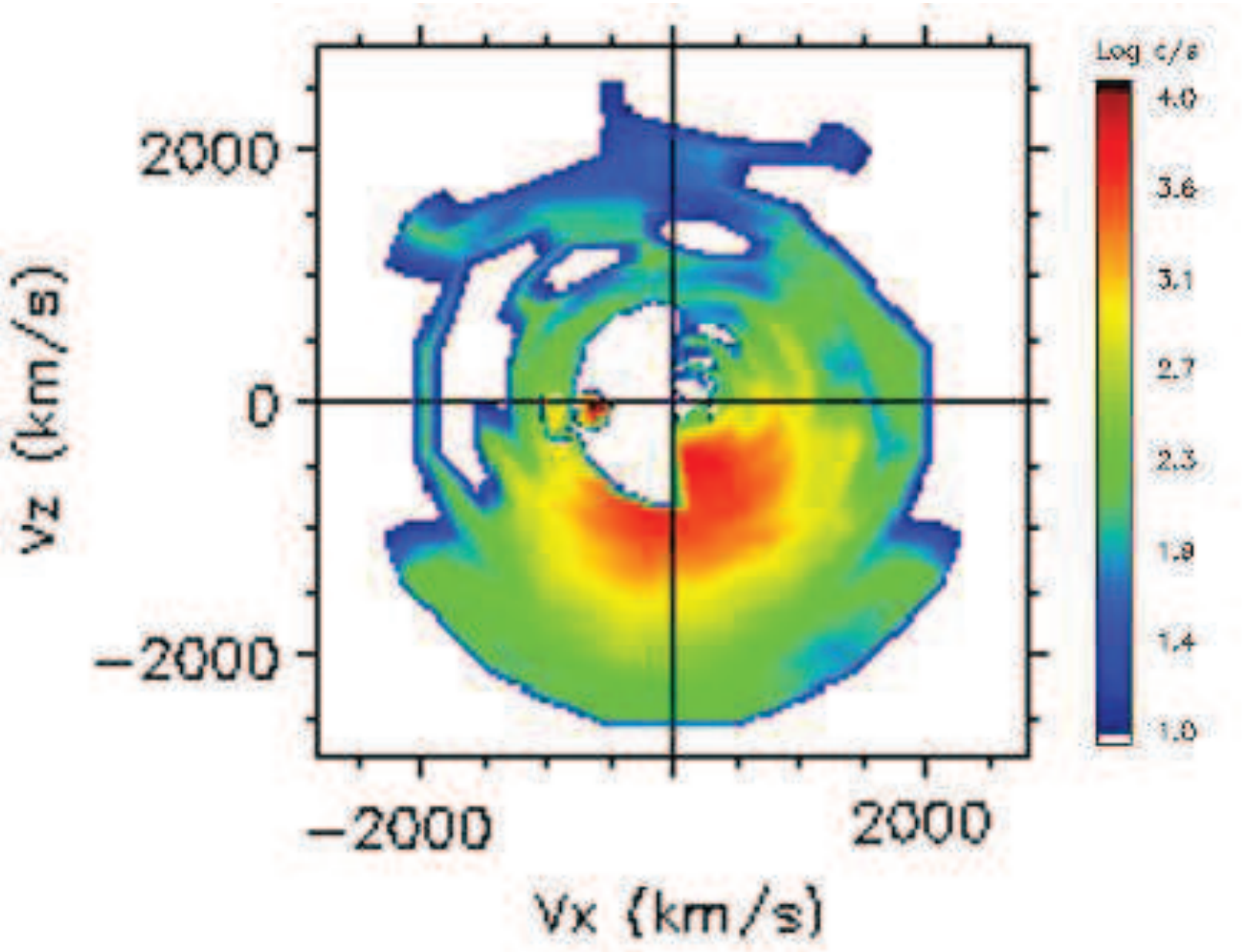

Figure4

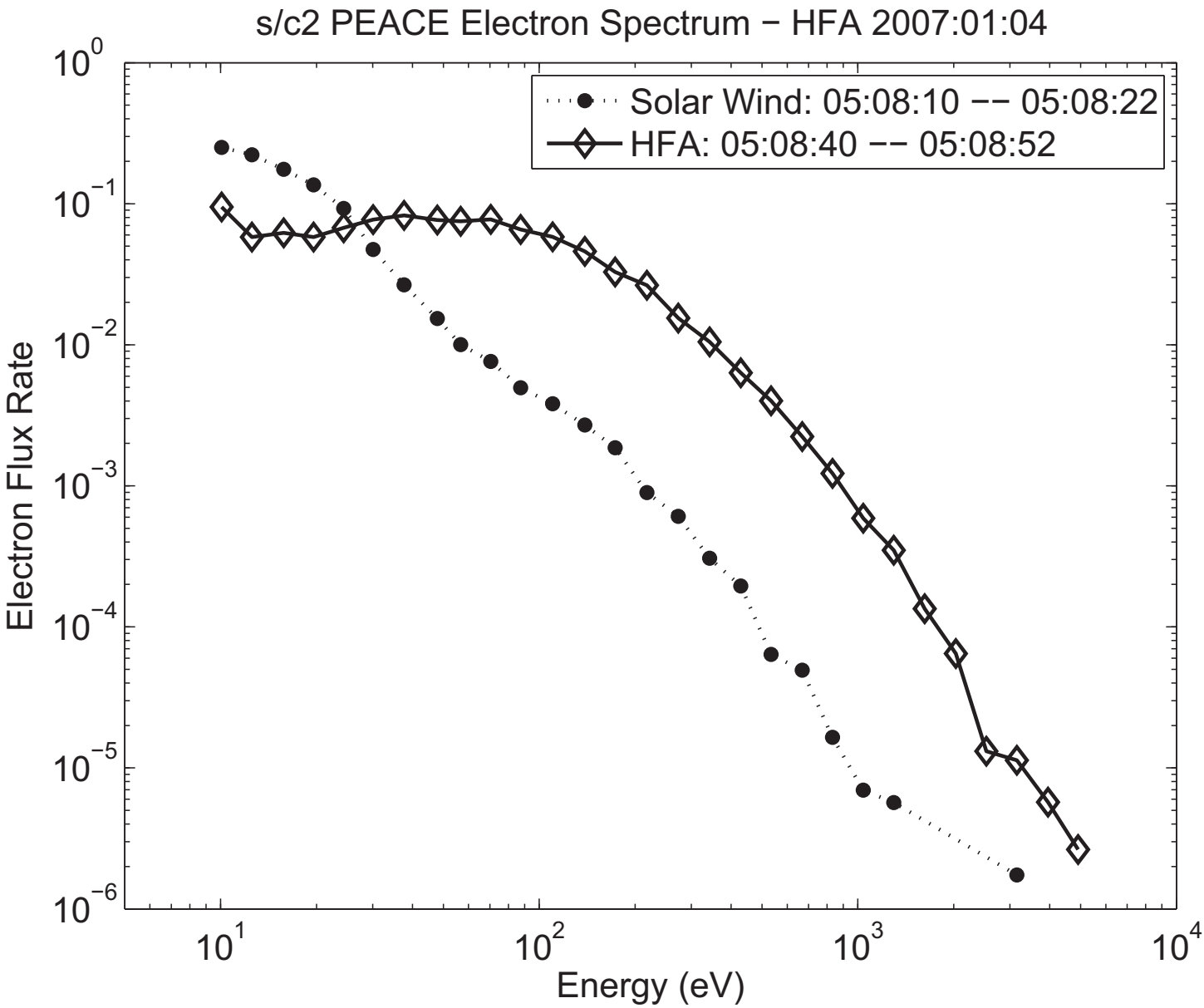
s/c2 PEACE Electron Spectrum − HFA 2007:01:04
Solar Wind: 05:08:10 −− 05:08:22
HFA: 05:08:40 −− 05:08:52
Electron Flux Rate
Energy (eV)
10^0
10^−1
10^−2
10^−3
10^−4
10^−5
10^−6
10^1
10^2
10^3
10^4

Figure5

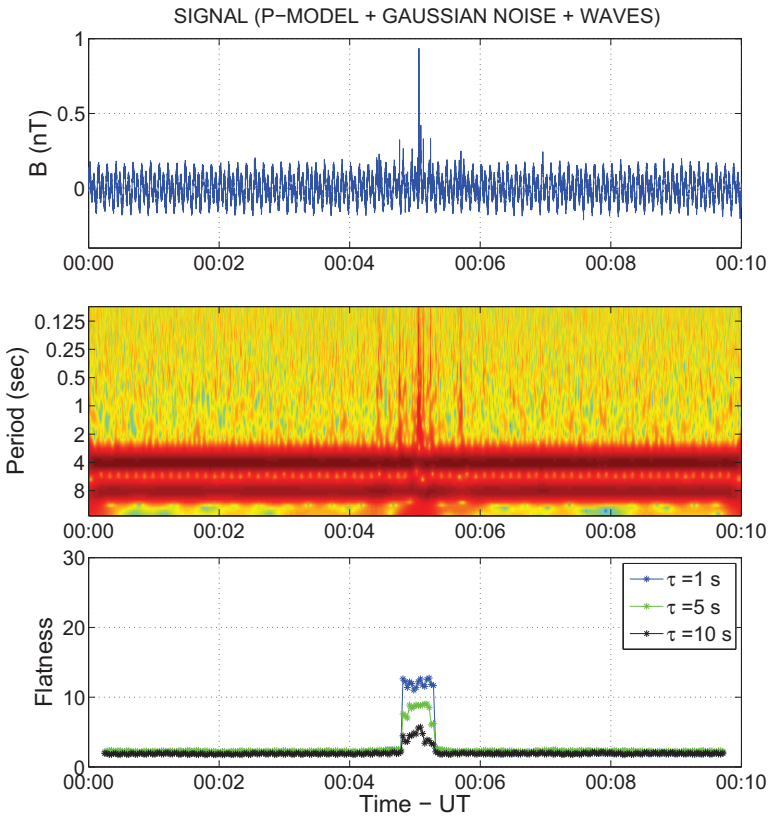
SIGNAL (P−MODEL + GAUSSIAN NOISE + WAVES)
B (nT)
Period (sec)
Flatness
τ =1 s
τ =5 s
τ =10 s
00:00
00:02
00:04
00:06
00:08
00:10
Time − UT

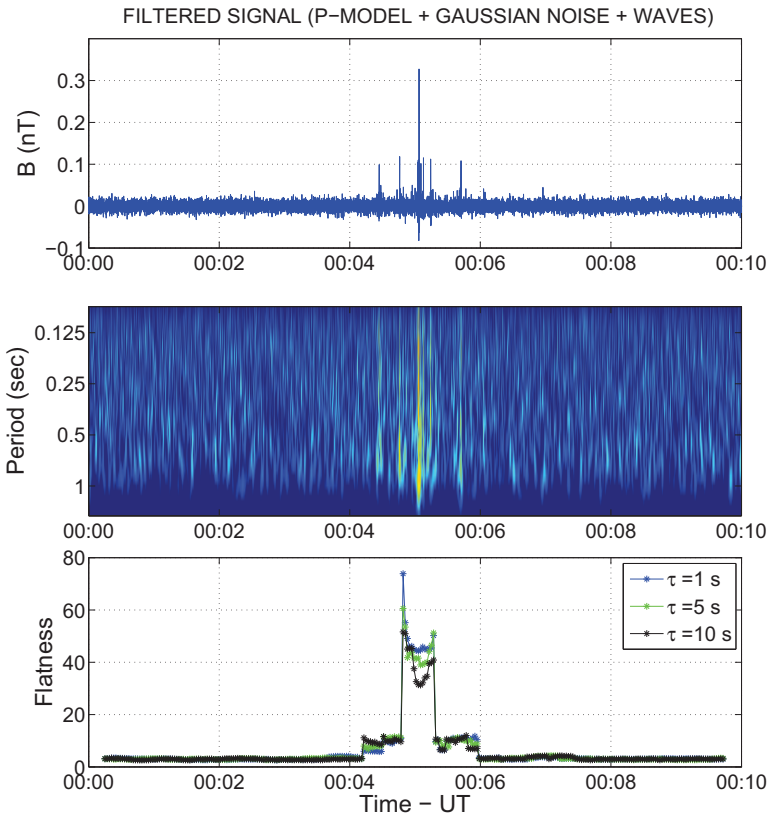
FILTERED SIGNAL (P−MODEL + GAUSSIAN NOISE + WAVES)
B (nT)
Period (sec)
Flatness
τ =1 s
τ =5 s
τ =10 s
00:00
00:02
00:04
00:06
00:08
00:10
Time − UT

Figure6

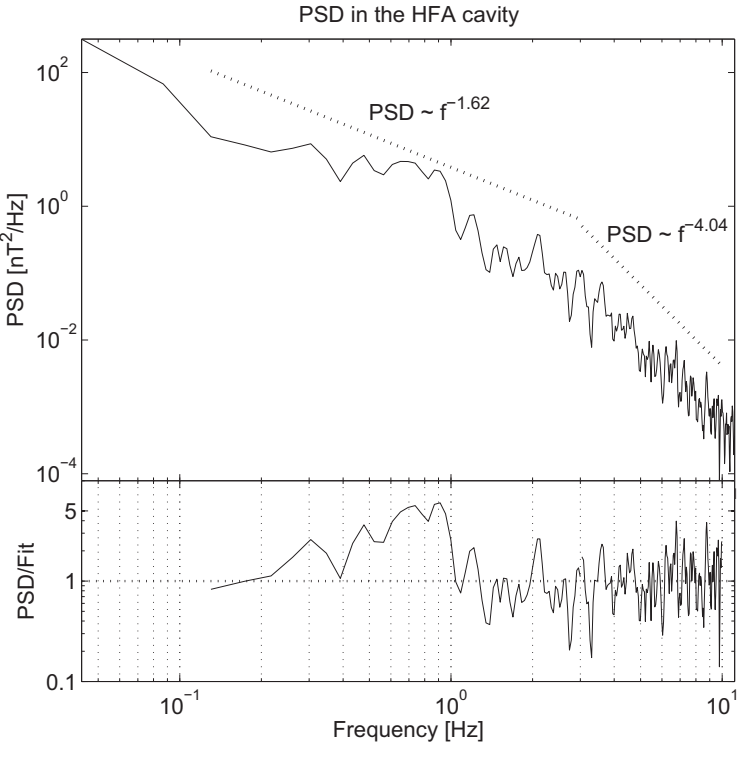
PSD in the HFA cavity
PSD ~ f^-1.62
PSD ~ f^-4.04
PSD [nT^2/Hz]
PSD/Fit
Frequency [Hz]

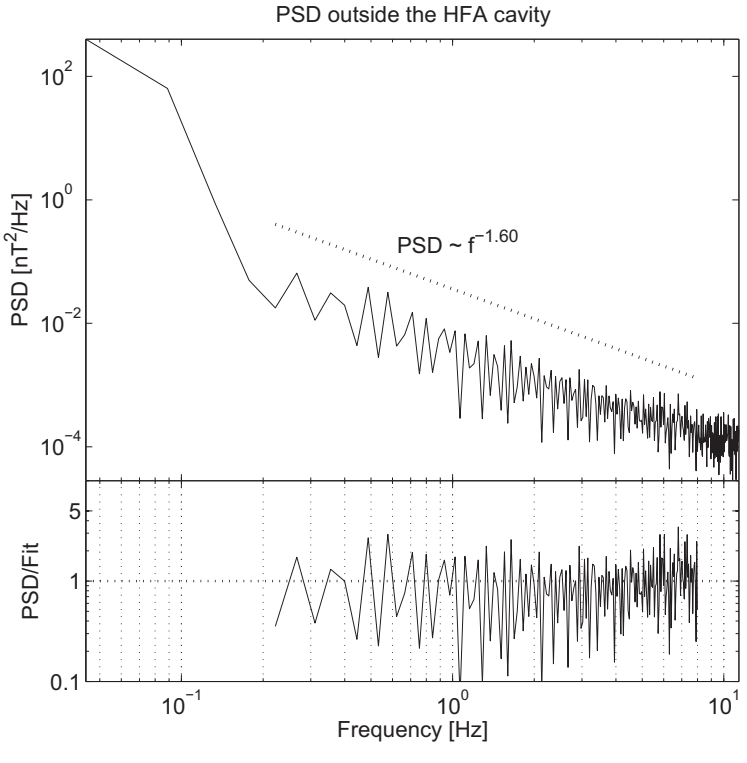
PSD outside the HFA cavity
PSD ~ f^-1.60
PSD [nT^2/Hz]
PSD/Fit
Frequency [Hz]

Figure7

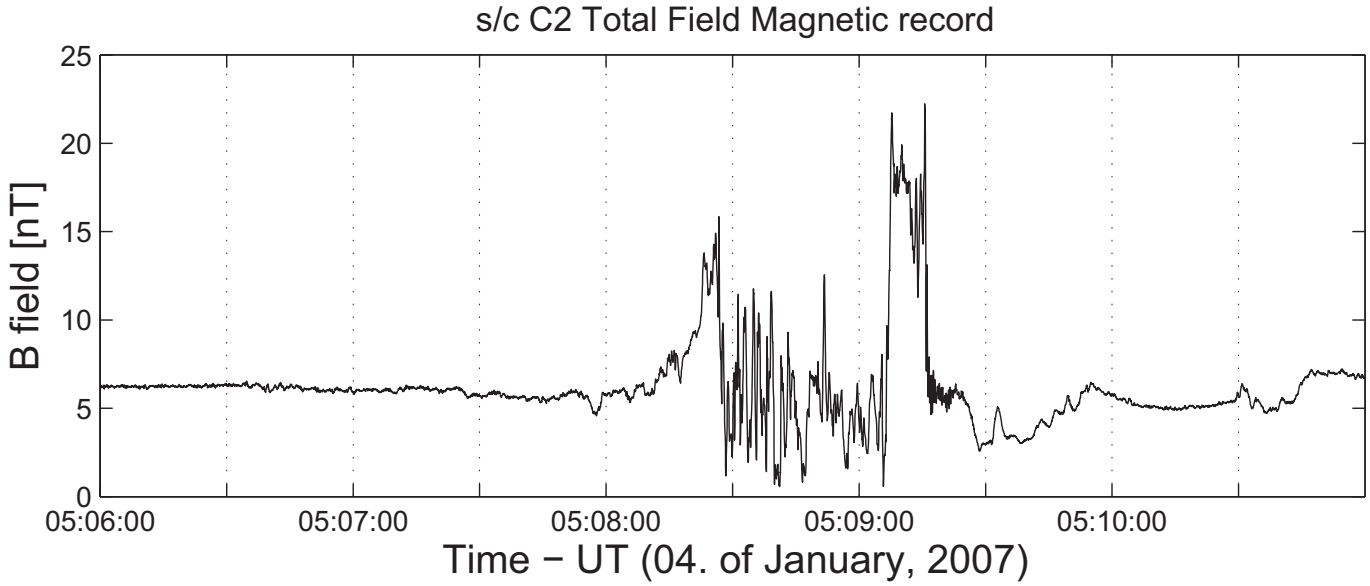
s/c C2 Total Field Magnetic record
B field [nT]
25
20
15
10
5
0
05:06:00
05:07:00
05:08:00
05:09:00
05:10:00
Time − UT (04. of January, 2007)

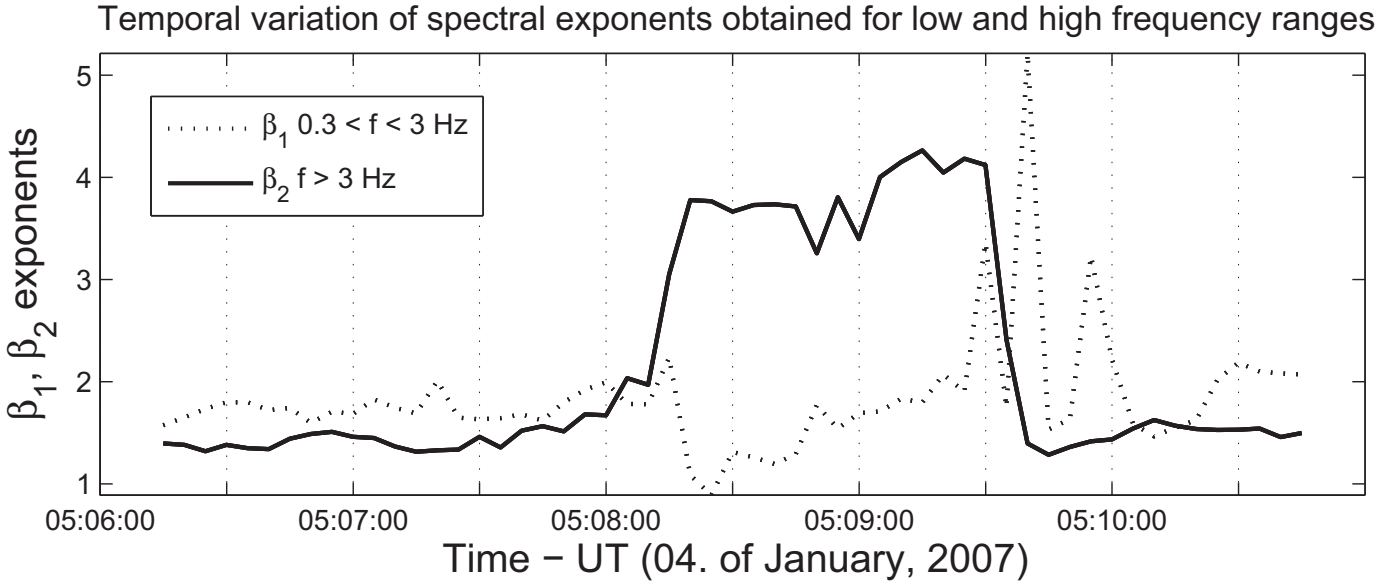
Temporal variation of spectral exponents obtained for low and high frequency ranges
β1 0.3 < f < 3 Hz
β2 f > 3 Hz
β1, β2 exponents
5
4
3
2
1
05:06:00
05:07:00
05:08:00
05:09:00
05:10:00
Time − UT (04. of January, 2007)

Figure8

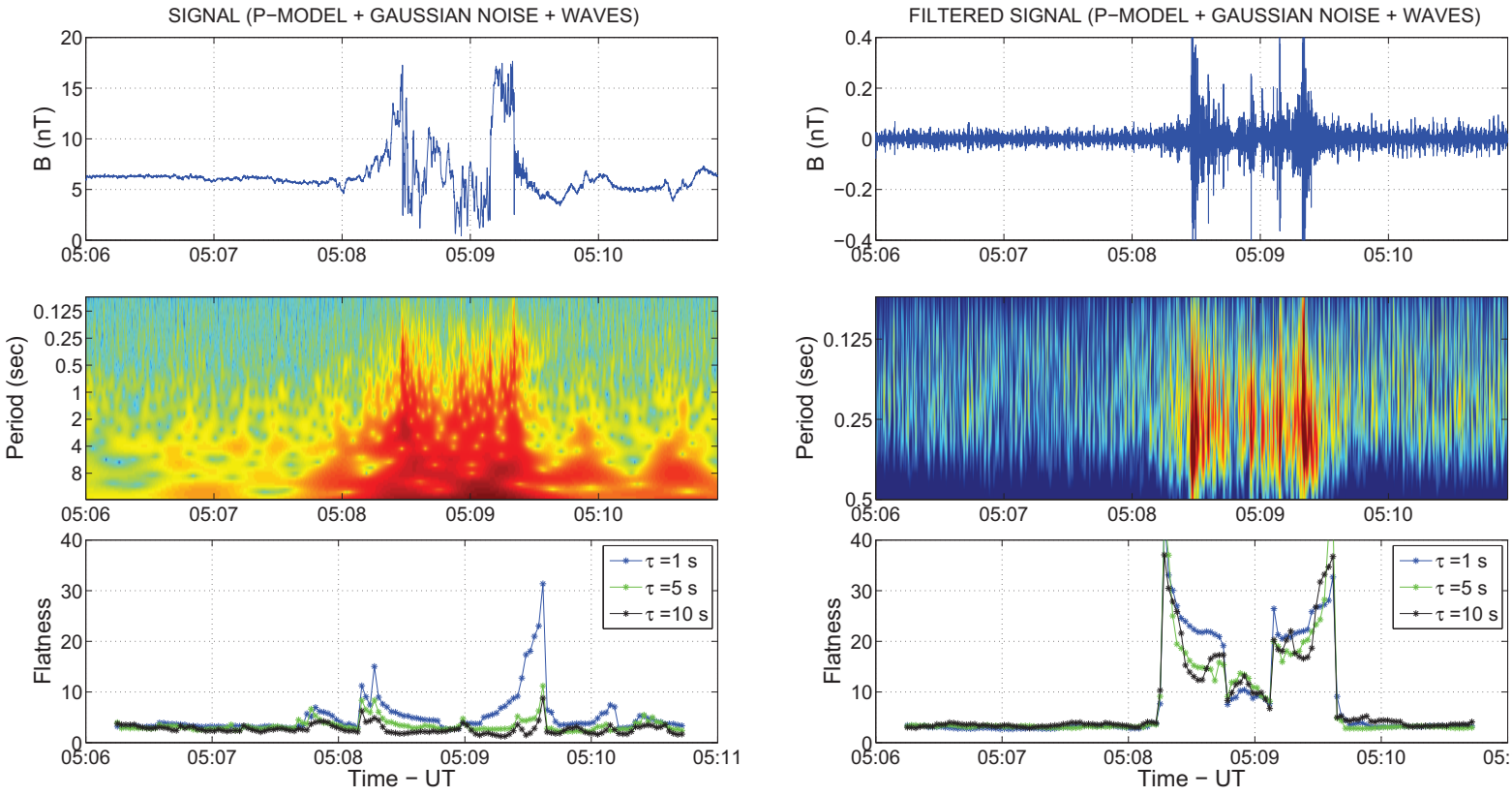
SIGNAL (P−MODEL + GAUSSIAN NOISE + WAVES)
FILTERED SIGNAL (P−MODEL + GAUSSIAN NOISE + WAVES)
B (nT)
Period (sec)
Flatness
τ =1 s
τ =5 s
τ =10 s
05:06
05:07
05:08
05:09
05:10
05:11
Time − UT

Figure9

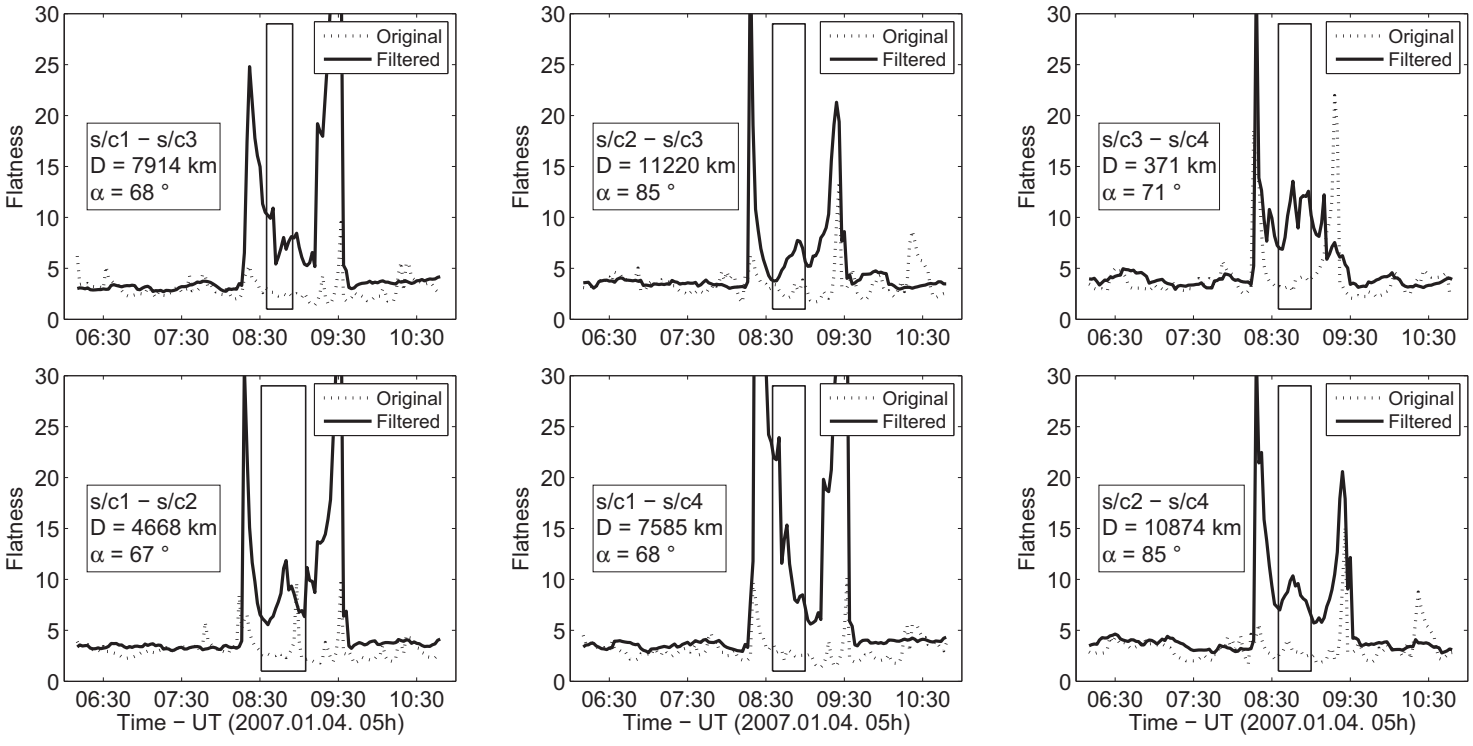
Original
Filtered
s/c1 − s/c3
D = 7914 km
α = 68 °
s/c2 − s/c3
D = 11220 km
α = 85 °
s/c3 − s/c4
D = 371 km
α = 71 °
s/c1 − s/c2
D = 4668 km
α = 67 °
s/c1 − s/c4
D = 7585 km
α = 68 °
s/c2 − s/c4
D = 10874 km
α = 85 °
Flatness
0
5
10
15
20
25
30
06:30
07:30
08:30
09:30
10:30
Time − UT (2007.01.04. 05h)